Analytical Biochemistry 411 (2011) 71–79

Contents lists available at ScienceDirect

Analytical Biochemistry

journal homepage: www.elsevier.com/locate/yabio

Electrocatalysis and simultaneous determination of catechol and quinol by poly(malachite green) coated multiwalled carbon nanotube film

Yogeswaran Umasankar, Arun Prakash Periasamy, Shen-Ming Chen *

Department of Chemical Engineering and Biotechnology, National Taipei University of Technology, Taipei 106, Taiwan, ROC

ARTICLE INFO

Article history:
Received 4 October 2010
Received in revised form 2 December 2010
Accepted 3 December 2010
Available online 5 December 2010

Keywords:
Multiwall carbon nanotubes
Malachite green
Modified electrodes
Electrocatalysis
Catechol
Quinol

ABSTRACT

Electrochemically active composite film that contains multiwalled carbon nanotubes (MWCNTs), Nafion (NF), and poly(malachite green) (PMG) has been synthesized on glassy carbon electrode (GCE), gold, and indium tin oxide (ITO) electrodes by potentiodynamic method. The presence of MWCNTs in the composite film (MWCNT–NF–PMG) enhances the surface coverage concentration (Γ) of PMG by fivefold. Similarly, an electrochemical quartz crystal microbalance study revealed enhancement in the deposition of PMG at MWCNT–NF film when compared with bare and only NF modified electrodes. The surface morphology of the composite film was studied using atomic force microscopy, which revealed that the PMG incorporated on MWCNT–NF film. The composite film exhibited enhanced electrocatalytic activity toward the mixture of biochemical compounds catechol and quinol. The electrocatalytic responses of analytes at MWCNT–NF–PMG composite film were measured using both cyclic voltammetry (CV) and differential pulse voltammetry (DPV). From electrocatalysis studies, well-separated voltammetric peaks were obtained at the composite film for catechol and quinol with a peak separation of 147 mV. The sensitivity values of the composite film toward catechol and quinol by the DPV technique were 0.4 and 3.2 mA mM^{-1} cm^{-2}, respectively, which are higher than the values obtained by the CV technique. Similarly, the above-mentioned values are better than the previously reported electroanalytical values for the same analytes.

Catechol and quinol are phenolic compounds and often coexist as isomers in environmental samples. Their crucial role in industrial applications causes their coexistence as environmental pollutants with high toxicity; therefore, several traditional and electrochemical methods have been developed for their determination [1–4]. When compared with several methods, the electrochemical method reduces the operating complexity, time, and reagents used for the determination of isomers. However, electrochemical analysis on unmodified electrodes, such as glassy carbon electrode (GCE)[1], has limitations because of the overlapping of oxidation potentials of catechol and quinol; hence, it often suffers from a pronounced fouling effect along with poor selectivity and reproducibility. Ghanem and others have overcome the above-mentioned problem by using chemically modified electrodes for the electrocatalysis and simultaneous determination of catechol and quinol [4–8].

Among the various preparation methods of chemically modified electrodes, electropolymerization is a simple but powerful method in targeting selective modification of different types of electrodes with desired matrices. The important advantages of electropolymerization are the easy synthesis and deposition of desired electroactive polymers onto the conductive surface from monomer solutions and the precise electrochemical control of their formation rate and thickness. These electroactive polymers have useful properties such as electronic conductivity and ionic conductivity [9]. As a consequence of all these above-mentioned advantages, the electropolymerization of electroactive polymers along with carbon nanotube (CNT) matrices has received considerable attraction during recent years. Numerous conjugated polymers have been electrochemically synthesized for their application in the fabrication of chemical and biochemical sensor devices [10–14]. These conjugated polymers used in sensor devices exhibit enhancement in the electrocatalytic activity toward the oxidation or reduction of several chemical and biochemical compounds [15] where some of the functional groups in polymers act as a catalyst [16,17]. In the current article, the term *enhanced electrocatalytic activity* is described as both an increase in peak current and lower overpotential [18]. The wide variety of applications of matrices made of CNTs for the detection of chemical and

* Corresponding author. Fax: +886 2270 25238.
E-mail address: smchen78@ms15.hinet.net (S.-M. Chen).

[1] *Abbreviations used:* GCE, glassy carbon electrode; CNT, carbon nanotube; MG, malachite green; PMG, poly(malachite green); FT-IR, Fourier transform infrared; UV–vis, ultraviolet–visible; MWCNT, multiwalled carbon nanotube; NF, Nafion; CV, cyclic voltammetry; EQCM, electrochemical quartz crystal microbalance; DPV, differential pulse voltammetry; AFM, atomic force microscopy; ITO, indium tin oxide; LOD, limit of detection; LOQ, limit of quantification.

0003-2697/$ - see front matter © 2010 Elsevier Inc. All rights reserved.
doi:10.1016/j.ab.2010.12.002

biochemical compounds has already been reported in the literature [19–22].

Even though the electrocatalytic activity of conjugated polymers and CNT matrices individually shows good results, new studies have been developed during the past decade for the preparation of composite films composed of both CNTs and conjugated polymers to improve matrix properties such as high sensitivity and good stability [23–25]. The incorporation of CNTs in conjugated polymers leads to the formation of new composite materials having the properties of each component with a synergistic effect that would be useful in particular applications [26]. These electroactive polymer/CNT composite matrices possess good solubility in organic solvents compared with unmodified CNTs. Moreover, polymer matrices exhibit high compatibility in the presence of CNTs [27]. There have been past attempts for the preparation of composite and sandwiched films made of polymer adsorbed on CNTs, and these were used for electrocatalysis studies such as selective detection of dopamine in the presence of ascorbic acid [28]. The sandwiched films were also used in the designing of nanodevices with the help of noncovalent adsorption, electrodeposition, and so forth [29].

Among the conjugated polymers, a group of them representing azines, such as phenazines, phenothiazines, and phenoxazines, have been widely used in bioelectrochemistry as redox indicators and mediators [30]. The electropolymerization of azine group compounds is usually performed by anodic oxidation in acidic medium [31,32]. Similar to these azine dyes, malachite green (MG) is also a dye compound that has an open but ionized structure; hence, the resulting polymer is promising in exhibiting interesting features such as fast rate of charge transfer and ion transport and good catalytic ability toward small biomolecules [33]. Previous studies have reported that poly(malachite green) (PMG) can be synthesized by electrochemical polymerization of MG. These studies also reported the growth mechanism of PMG along with electrochemical, Fourier transform infrared (FT-IR), and ultraviolet–visible (UV–vis) studies [33–35]. The chemical structures of MG and PMG are shown in Scheme 1.

In this article, we report a novel composite film, MWCNT–NF–PMG, made of multiwalled carbon nanotubes (MWCNTs) that were dispersed using Nafion (NF) and then incorporated with PMG. MWCNT–NF–PMG composite film's characterization, enhancement in functional properties, peak current, and electrocatalytic activity are also reported along with its application in the simultaneous determination of catechol and quinol. When compared with previously reported analytical values, MWCNT–NF–PMG composite film modified electrode has enhanced electrocatalysis of catechol and quinol [4,6–8]. The MWCNT–NF–PMG film preparation involves two steps: (i) electrodes are modified with uniformly well-dispersed MWCNT–NF, (ii) which is then modified with PMG.

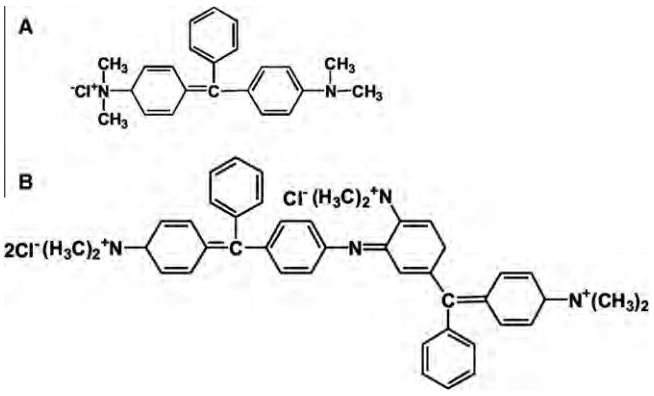

Scheme 1. Chemical structures of MG (A) and PMG (B).

Materials and methods

Materials

MG, NF, MWCNTs (outer diameter = 10–20 nm, inner diameter = 2–10 nm, length = 0.5–200 μm), catechol, and quinol obtained from Aldrich and Sigma–Aldrich were used as received. All other used chemicals were of analytical grade. The preparation of aqueous solution was done with double distilled deionized water. Solutions used for the experiments were deoxygenated by purging with prepurified nitrogen gas. The pH 1.5 aqueous solution was prepared from H_2SO_4.

Apparatus

Cyclic voltammetry (CV), electrochemical quartz crystal microbalance (EQCM), and differential pulse voltammetry (DPV) studies were performed using analytical system models CHI-405, CHI-400, and CHI-750 potentiostats, respectively. A conventional three-electrode cell assembly consisting of an Ag/AgCl reference electrode and a platinum wire counter electrode were used for the electrochemical measurements. The working electrode was GCE modified with PMG, NF–PMG, or MWCNT–NF–PMG composite films. In these experiments, all of the potentials are reported versus Ag/AgCl reference electrode. The working electrode for EQCM measurements was an 8-MHz AT-cut quartz crystal coated with a gold electrode. The diameter of the quartz crystal was 13.7 mm, and that of the gold electrode was 5 mm. The morphological characterizations of the films were examined by means of atomic force microscopy (AFM) (Being Nano-Instruments CSPM-4000). All of the measurements were carried out at 25 ± 2 °C.

Preparation of MWCNT–NF–PMG composite electrodes

The important challenge in the dispersion of MWCNTs was preparation of a homogeneous solution. In general, the dispersion of CNTs has been carried out by physical (milling) and chemical methods (covalent and noncovalent functionalization). These methods cause damage to CNTs and add impurities to them [36,37]. To overcome these drawbacks, hydrophobic interaction between NF and MWCNTs was used for our experiments [38,39]. Briefly, the dispersion of MWCNTs was done by using 5% NF (2 ml of NF in 10 ml of water) with 10 mg of MWCNTs (MWCNT–NF). The uniform dispersion of MWCNTs was obtained by 6 h of ultrasonication of MWCNT–NF mixture.

Before starting each experiment, GCEs were polished using a BAS polishing kit with 0.05 μm alumina slurry and then rinsed and ultrasonicated in double distilled deionized water. The GCEs studied were uniformly coated with 10 μl of MWCNT–NF mixture (0.13 mg cm^{-2} MWCNTs) and dried at room temperature. Then MG was electropolymerized on the MWCNT–NF modified GCE from 5 mM MG present in pH 1.5 H_2SO_4 aqueous solution. The electropolymerization was performed by consecutive cyclic voltammograms (25 cycles) over an optimized potential range of 0–1.2 V at a scan rate of 100 mV s^{-1}. After that, the modified MWCNT–NF–PMG electrode was carefully washed with double distilled deionized water.

Results and discussion

Electropolymerization of MG at various electrodes and their characterizations

The electropolymerization of MG (from 5 mM MG solution) using electrochemical oxidation on unmodified, MWCNT–NF

modified, and only NF modified GCEs was performed for the preparation and comparative studies of PMG, NF–PMG, and MWCNT–NF–PMG composite films. During electropolymerization, on subsequent cycles the redox peak corresponding to PMG was found to be increasing in all of the above-mentioned films (not shown). This result indicates that during the cycles, deposition of PMG takes place on the electrode surface. However, the redox peak of PMG at bare GCE is not highly active when compared with the other two electrodes. The above-prepared three films (PMG, NF–PMG, and MWCNT–NF–PMG) were characterized using various electrochemical techniques in pH 1.5 H_2SO_4 aqueous solution. Before transferring the modified GCEs to aqueous solution for other electrochemical characterizations, they were washed carefully in deionized water to remove the loosely attached nonpolymerized MG monomer on the modified GCEs. Fig. 1A shows the reversible redox couple of PMG at NF modified and MWCNT–NF modified GCEs, whereas there is no redox couple at bare GCE. The corresponding cyclic voltammograms were measured at a scan rate of 20 mV s^{-1} in the potential range of 0.85–0.20 V. Among these three films, the $E^{0'}$ value of the redox couple for MWCNT–NF–PMG composite film is at 559 mV versus Ag/AgCl in pH 1.5 H_2SO_4 aqueous solution, where the redox couple represents the redox reaction of PMG. The E_{pa}, E_{pc}, and I_{pc} values of PMG at various film modified electrodes are given in Table 1. Interestingly, the values in Table 1 reveal that MWCNT–NF modified GCE has a higher polymerizing current for PMG than at other modified or unmodified GCEs. The above results represent more deposition of PMG on MWCNT–NF modified GCE than on other GCEs.

The increase in deposition of PMG in the presence of MWCNTs is evident with the active surface coverage concentration (Γ) given in Table 1, where Γ of PMG is enhanced at MWCNT–NF film modified GCE when compared with only NF modified and bare GCEs. The calculated values from the same table show that MWCNTs enhance Γ of PMG by 238 nmol cm^{-2} μg^{-1}, and there is a fivefold increase in the Γ of PMG at MWCNT–NF film. In these Γ calculations, the number of electrons involved in PMG redox reactions is assumed to be two. A comparison of PMG, NF–PMG, and MWCNT–NF–PMG films on gold and indium tin oxide (ITO) electrodes is given in the Supplementary material. In the above experiments as well, MWCNT modified electrodes show a higher polymerizing current for PMG than at other modified and unmodified electrodes, consistent with the I_{pc} and Γ values given in Table 1. The possible interactions among MWCNTs, NF, and PMG present in the composite film are given in Scheme 2, where the interaction between MWCNTs and NF is hydrophobic and the interaction between NF and PMG is both hydrophobic and electrostatic.

Table 1
E_{pa}, E_{pc}, and I_{pc} values of redox reactions of PMG and surface coverage concentration (Γ) of PMG at various modified electrodes present in pH 1.5 H_2SO_4 aqueous solution.

Modified electrodes		E_{pa} (V)	E_{pc} (V)	I_{pc} (μA)	Γ (nmol cm^{-2})
Electrode	Film				
GCE	PMG[a]	0.61	0.5	−186.9	38.13
	PMG[b]	0.62	0.5	−38.98	7.19
	PMG	–	–	–	–
Gold	PMG[a]	0.67	0.5	−32.48	14.97
	PMG[b]	–	0.43	−5.187	3.55
	PMG	0.67	0.47	−0.131	0.10
ITO	PMG[a]	0.63	0.49	−249.5	9.02
	PMG[b]	–	0.42	−31.27	1.21
	PMG	0.65	0.4	−0.173	0.008

[a] PMG electropolymerized on MWCNT–NF modified electrode.
[b] PMG electropolymerized on NF modified electrode.

The MG electropolymerization was further confirmed using EQCM experiments, which were carried out using unmodified gold or modifying the gold in electrochemical quartz crystal with uniformly coated MWCNT–NF or only NF. The increase in voltammetric peak current of PMG redox couple and the frequency decrease (or mass increase) were found to be consistent with the growth of PMG film on bare gold electrode or on MWCNT–NF or NF modified gold electrodes (not shown). These results also show that the obvious deposition potential started between 0 and 1.2 V. From the frequency change, the change in mass of composite film at the quartz crystal can be calculated using the Sauerbrey equation (Eq. (1)); however, a 1-Hz frequency change is equivalent to 1.4 ng cm^{-2} mass change [40,41]. The mass changes during PMG incorporation on MWCNT–NF modified, NF modified, and unmodified gold electrodes for total cycles are 207, 70, and 52 ng cm^{-2}, respectively:

$$\text{mass change}(\Delta m) = -1/2(f_0^{-2})(\Delta f)A(K\rho)^{1/2} \quad (1)$$

where f_0 is the oscillation frequency of the crystal, Δf is the frequency change, A is the area of gold disk, K is the shear modulus

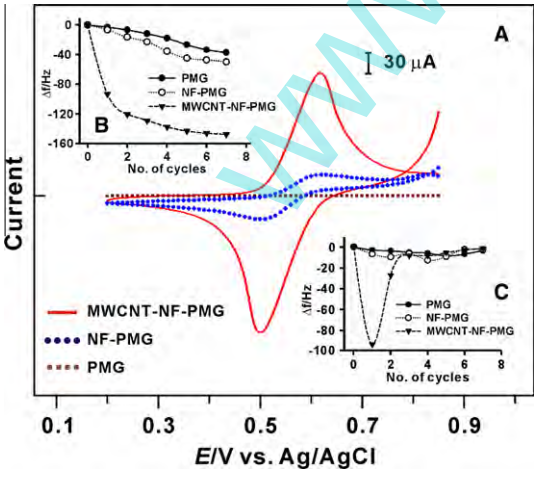

Fig.1. (A) Cyclic voltammograms of GCE modified from PMG, NF–PMG, and MWCNT–NF–PMG films in pH 1.5 H_2SO_4 solution at a scan rate of 20 mV s^{-1}. (B and C) EQCM frequency change responses recorded together with consecutive cyclic voltammograms (PMG formation on NF modified, MWCNT–NF modified, and unmodified gold electrodes, potential between 0 and 1.2 V at a scan rate of 20 mV s^{-1}), where panel B shows the gross change in the frequency shift versus scan cycles and panel C shows the change between each consecutive scan.

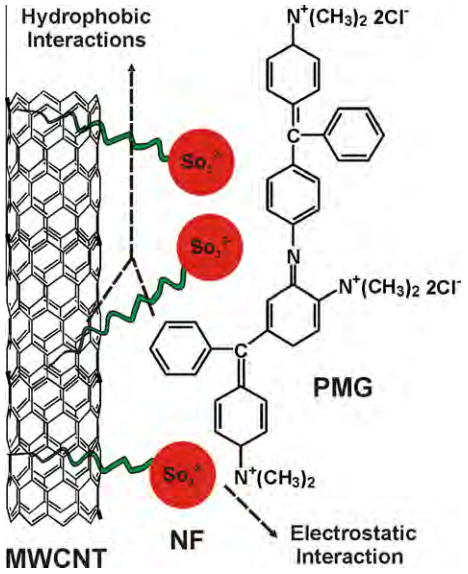

Scheme 2. Possible interactions among MWCNTs, NF, and PMG present in MWCNT–NF–PMG composite film.

of the crystal, and ρ is the density of the crystal. Fig. 1B indicates the variation of frequency with an increase of scan cycles for PMG at bare gold electrode and at NF modified and MWCNT–NF modified gold electrodes. This result proves that the deposition of PMG on the MWCNT–NF film is a higher concentration than that on NF modified or bare gold electrodes. Fig. 1C indicates every cycle of frequency with an increase of scan cycles for PMG at bare gold electrode and at NF modified and MWCNT–NF modified gold electrodes. This result shows that the rate of PMG deposition at MWCNT–NF film is high during the first cycle when compared with that for the other two films, whereas from the second cycle the rate of PMG deposition is equal for all three films.

AFM studies of MWCNT–NF, NF–PMG, and MWCNT–NF–PMG composite films

MWCNT–NF, NF–PMG, and MWCNT–NF–PMG were prepared with similar conditions and similar potential, as mentioned in Materials and Methods, and were characterized using AFM. A comparison of Fig. 2A, B, and C reveals a significant morphological difference among all three films. The top views of nanostructures in Fig. 2A on the ITO electrode surface shows the presence of clusters of NF together with MWCNTs. The NF–PMG film in Fig. 2B shows smaller beads of NF and PMG deposited over the electrode surface. However, there are no bead formations if only NF is coated over the electrode; instead, a porous NF film is formed. Similarly, a uniform thin film with no morphology is formed for only PMG deposited over the electrode surface [35]. The MWCNT–NF–PMG composite film in Fig. 2C shows plateaus of PMG formed over MWCNT–NF film. Furthermore, in Fig. 2C, MWCNTs are not obviously visible as they are in Fig. 2A because PMG deposition covers over MWCNTs. The results in Fig. 2C can be explained as the increase in deposition of PMG over MWCNT–NF, which creates plateaus instead of beads and covers over MWCNTs. The higher concentration of PMG deposited on MWCNT modified ITO electrode when compared with other modified electrodes is consistent with the Γ values shown in Table 1. Furthermore, the thicknesses of MWCNT–NF, NF–PMG, and MWCNT–NF–PMG obtained using AFM results were 350, 180, and 900 nm, respectively. These values also show that MWCNT–NF–PMG has higher thickness than the other two films. To further confirm the results, AFM amplitude images are included for these three films in Fig. 2D, E, and F, respectively. These AFM results reveal the coexistence of MWCNT–NF and PMG in the composite film.

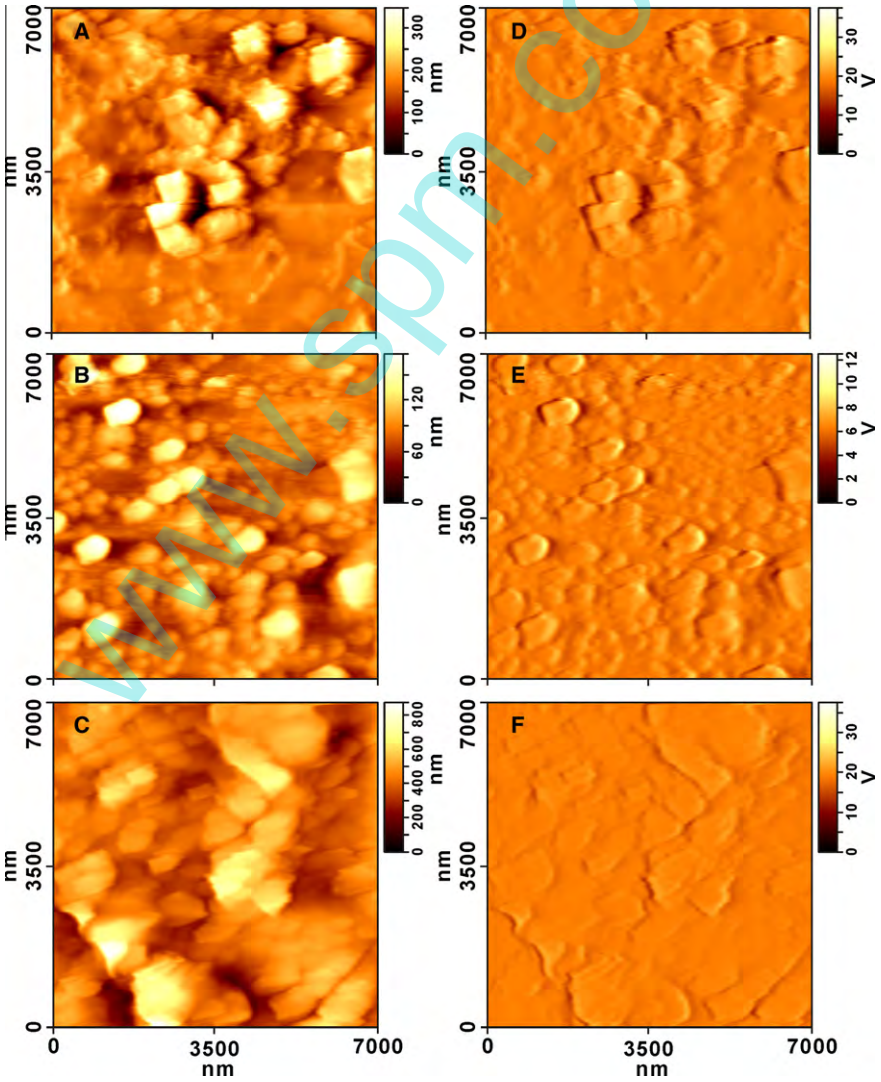

Fig.2. (A–C) AFM topography images of MWCNT–NF (A), NF–PMG (B), and MWCNT–NF–PMG (C) films. (D–F) AFM amplitude images of MWCNT–NF (D), NF–PMG (E), and MWCNT–NF–PMG (F) films.

Electrochemical and stability studies of MWCNT–NF–PMG composite film

The cyclic voltammograms of MWCNT–NF–PMG composite film on GCE in pH 1.5 H_2SO_4 aqueous solution at different scan rates show that the anodic and cathodic peak currents of the composite film's redox couple increases linearly with the increase of scan rates (not shown). The I_{pa}/I_{pc} ratio for MWCNT–NF–PMG film is small, demonstrating that the redox process is surface confined. However, the ΔE_p of each scan rate reveals that the peak separation of MWCNT–NF–PMG film's redox couple increases as the scan rate increase. From the slope values of ΔE versus log scan rate, by assuming the value of $\alpha \approx 0.5$ and the number of electrons involved as two, the electron transfer rate constant (k_s) was calculated using the Eq. (2) based on Laviron's theory [42]:

$$\log ks = \alpha \log(1-\alpha) + (1-\alpha)\log\alpha - \log(RT/nFv) - \alpha(1-\alpha)nF\Delta E/2.3RT. \quad (2)$$

In Eq. (2), the scan rate and ΔE values are in unit volts. The k_s value of MWCNT–NF–PMG modified GCE is 18.3 ms^{-1}. Fig. 3A shows the cyclic voltammograms of MWCNT–NF–PMG modified GCE in various pH aqueous buffer solutions, where the film was prepared in pH 1.5 H_2SO_4 aqueous solution and then washed with deionized water before transferring to various pH solutions. The results show that the film is stable in the pH range between 1.5 and 13.0; however, there is no redox activity of PMG in alkaline pH. The values of E_{pa} and E_{pc} depend on the pH value of buffer solution. The inset in Fig. 3A shows the formal potential of MWCNT–NF–PMG plotted over the pH range from 1.5 to 13.0. The slope value is −35 mV pH^{-1}, which is close to that given by the Nernstian equation for nonequal number of electrons and protons transfer.

The enhancement in stability of PMG in the presence of MWCNTs was examined, and the percentages of degradation of MWCNT–NF–PMG and NF–PMG were calculated using an equation given in previous literature [43,44]. The experimental results in Fig. 3B display the successive 280 min of cycling (scan rate = 20 mV s^{-1}) applied over the potential range of 0.2–0.8 V on MWCNT–NF–PMG and NF–PMG in pH 1.5 H_2SO_4 aqueous solution. The cyclic voltammograms were recorded at an interval of 30 min each, and the values of I_{pc} were plotted against time. From these results, it is clear that after 200 min the response of MWCNT–NF–PMG becomes constant with time and cycling, indicating that it is a stable film. However, the NF–PMG continues to degrade on cycling. The amounts of degradation after 280 min of cycling for MWCNT–NF–PMG and NF–PMG are 12 and 48%, respectively. From the above result, the percentage decrease in degradation of PMG in the presence of MWCNTs is approximately 36% for 280 min of cycling. Similar enhancements in CNTs with polymer composite properties when compared with CNT or polymer alone have already been reported in the literature [26,27].

Electroanalysis of catechol and quinol individually at PMG, NF–PMG, and MWCNT–NF–PMG film modified GCEs

The electrochemical oxidation of catechol and quinol at different film modified GCEs was carried out using pH 1.5 H_2SO_4 solution at 20 mV s^{-1} in the potential range of 0.10–0.85 V (see Supplementary material). The different electrodes used were bare GCE and PMG, NF–PMG, and MWCNT–NF–PMG composite film modified GCEs. All of the cyclic voltammograms were recorded at a constant time interval of 2 min with nitrogen purging before the start of each experiment. The cyclic voltammograms for NF–PMG and MWCNT–NF–PMG films exhibit a redox couple in the absence of analytes, whereas no redox peak for bare and PMG modified GCEs is observed. In the presence of analytes, new

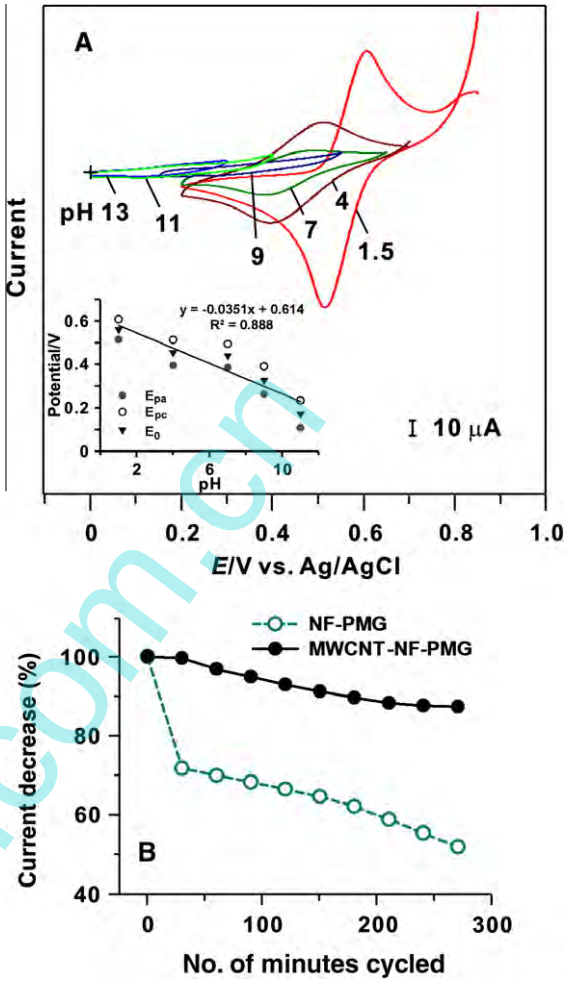

Fig.3. (A) Cyclic voltammograms of MWCNT–NF–PMG film synthesized using pH 1.5 H_2SO_4 solution on GCE and transferred to various pH solutions. The inset shows E_{pa}, E_{pc}, and the formal potential versus pH from 1.5 to 13.0 (slope = −35 mV/pH), where the slope is almost nearer the Nernstian equation for nonequal number of electrons and protons transfer. (B) Number of minutes cycled versus current decrease (in %) for NF–PMG and MWCNT–NF–PMG films, showing that MWCNT–NF–PMG is highly stable when compared with NF–PMG film.

growth in the oxidation peaks of respective analytes appears. The E_{pa} and I_{pa} values of analytes at different modified and unmodified GCEs are given in Table 2. The I_{pa} values reveal that MWCNT–NF–PMG film modified GCE has a higher peak current than the other modified and unmodified GCEs. Similarly, among the E_{pa} values, MWCNT–NF–PMG film shows a new peak at 302 mV for catechol that is not present at other modified and unmodified GCEs. Both this decrease in overpotential and the increase in peak current are considered as enhancement of electrocatalysis [18]. Furthermore, MWCNT–NF–PMG film has catechol's peak current at a lower positive potential than that of quinol. Among the E_{pa} values, 302 mV (catechol) and 449 mV (quinol) peaks were chosen for further investigation. The above-mentioned peaks were chosen because of their lower overpotential and the obvious peak potential difference of 147 mV between catechol and quinol.

An increase in concentration of catechol or quinol simultaneously produces a linear increase in the oxidation peak currents of respective analyte at MWCNT–NF–PMG film, as shown in the inset plots in the Supplementary material. However, there is no increase in the analyte oxidation peak currents at bare GCE and PMG and NF–PMG modified GCEs. From the slopes, the sensitivity values of MWCNT–NF–PMG film modified GCE toward the analytes were

Table 2
Electroanalytical results for catechol and quinol individually and in mixture at various modified GCEs using the CV technique in pH 1.5 H_2SO_4 solution.

Analyte			E_{pa} (mV)	I_{pa} (μA)	Concentration range (μM)		Sensitivity (mA mM^{-1} cm^{-2})
					Lowest	Highest	
Individual	Catechol	[a]	724	99.10	–	3921.0[e]	–
		[b]	757	24.23	–	740.7[e]	–
		[c]	740	54.37	–	2063.5[e]	–
		[d]	302, 623	19.34, 225.4	49.8	3650.8	0.08
	Quinol	[a]	593	110.4	–	3921.0[e]	–
		[b]	723	44.25	–	2156.9[e]	–
		[c]	548, 680	11.62, 17.45	–	2156.9[e]	–
		[d]	449, 621	43.83, 211.0	49.8	3921.0	0.22
Mixture	Catechol	[d]	302	20.06	184.7	4054.1	0.07
	Quinol	[d]	449	32.06	73.9	1621.6	0.23

[a] Bare GCE.
[b] PMG modified GCE.
[c] NF–PMG modified GCE.
[d] MWCNT–NF–PMG modified GCE.
[e] No increase in oxidation peak of respective analyte.

calculated and are given in Table 2. The correlation coefficients are 0.9831 and 0.992 for catechol and quinol, respectively. These sensitivity values and the I_{pa} values show that the peak currents of both analytes are high at MWCNT–NF–PMG composite film when compared with other modified and unmodified GCEs. The calculated limits of detection (LODs) at MWCNT–NF–PMG are 31.0 μM for catechol and 18.1 μM for quinol individually. The above results reveal that the enhanced electrocatalysis of both analytes takes places at MWCNT–NF–PMG film when compared with other GCEs.

Voltammetric resolution of analytes present in the mixture at PMG, NF–PMG, and MWCNT–NF–PMG film modified GCEs

Fig. 4 shows the electrochemical oxidation cyclic voltammograms that were obtained for catechol and quinol coexisting (analyte mixture) at bare GCE and PMG, NF–PMG, and MWCNT–NF–PMG film modified GCEs in pH 1.5 H_2SO_4 solution at 20 mV s^{-1} in the potential range of 0.10–0.85 V. The MWCNT–NF–PMG film is given in the presence and absence of analyte mixture. Bare GCE and PMG and NF–PMG modified GCEs are given at the highest concentration of analyte mixture. The lowest and highest concentrations of the analyte mixture are given in Table 2. The cyclic voltammograms of bare GCE and PMG and NF–PMG film modified GCEs in Fig. 4 exhibit only one broad peak in high potential without any peak separation for the analyte mixture. Here the broad peak represents the voltammetric signals of the analyte mixture. Moreover, the peak current decreases in the subsequent cycles for all three of these GCEs. These observations indicate that bare GCE and PMG and NF–PMG film fail to separate the voltammetric signals of analytes in the mixture. The fouling effect of the electrode surface with the oxidized products of analytes is the reason for obtaining the weak single peak for analytes in the mixture [4,5]. The cyclic voltammogram for MWCNT–NF–PMG exhibits a redox couple in the absence of the analyte mixture. In the presence of the analyte mixture, new growth in the oxidation peaks of respective analytes appears at the E_{pa} values given in Table 2. From these E_{pa} values, the peak separation between catechol and quinol at MWCNT–NF–PMG composite film was calculated as 147 mV. An increase in concentration of analyte mixture simultaneously produces a linear increase in the oxidation peak currents of both analytes with good film stability, as shown in the Fig. 4 insets.

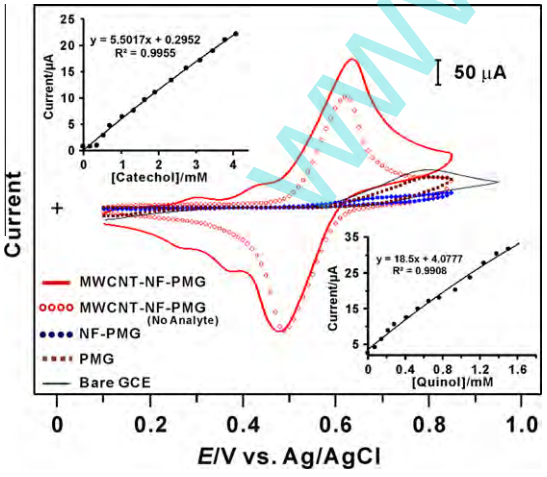

Fig.4. Cyclic voltammograms of catechol and quinol present in analyte mixture at various electrodes using pH 1.5 H_2SO_4 solution at 20 mV s^{-1}, where MWCNT–NF–PMG is shown in the presence and absence of analytes. Similarly, bare GCE, PMG modified, and NF–PMG modified GCEs are shown in the presence of the highest concentration of analyte mixture, where the concentration range is given in Table 2. The insets show the plots of peak current versus concentration of catechol (upper left) and quinol (lower right) at MWCNT–NF–PMG.

The I_{pa} values from Table 2 show that the anodic peak current of both analytes at MWCNT–NF–PMG is higher than that at other film modified and unmodified GCEs. In these results, both the increase in current and the decrease in potential are considered as the enhancement of electrocatalysis [18]. The electroanalytical values such as linear range, slope and its correlation coefficient, standard error of slope, LOD, and limit of quantification (LOQ) for the analyte mixture at MWCNT–NF–PMG film are given in Table 3. From the slope values, sensitivity values of the MWCNT–NF–PMG film modified GCE were calculated and are given in Table 2. From all of the above results, it is obvious that MWCNT–NF–PMG composite film is more efficient for the simultaneous determination of catechol and quinol present in the mixture.

DPV studies of catechol and quinol at MWCNT–NF–PMG composite film

The differential pulse voltammograms were obtained with an increase in catechol and quinol concentrations individually at MWCNT–NF–PMG composite film modified GCE in pH 1.5 H_2SO_4 solution (see Supplementary material). All of the differential pulse voltammograms were recorded at a constant time interval of 2 min with nitrogen purging before the start of each experiment. The peak currents for both catechol and quinol increase linearly with the increase in concentration of respective analytes. They demonstrate that the calibration curves for both analytes are linear for a

Table 3
Electroanalytical results for catechol and quinol present in mixture at MWCNT–NF–PMG composite film using the CV and DPV techniques in pH 1.5 H_2SO_4 solution.

Analyte	Catechol		Quinol	
	CV	DPV	CV	DPV
Linear range (mM)	0.36–4.05	0.03–1.19	0.22–1.62	0.01–0.48
Slope (μA mM^{-1})/correlation coefficient	5.502/0.9955	27.71/0.9514	18.5/0.9908	256.29/0.9596
Standard error of slope	0.1020	1.0823	0.4944	6.8796
Intercept (μA)	0.2952	19.539	4.0777	22.092
LOD (μM)	29.3	5.8	22.3	1.6
LOQ (μM)	88.8	17.6	67.4	4.8

wide range of concentrations—from 0.4 to 1.3 mM for catechol and from 0.4 to 1.0 mM for quinol. From the slope values, the sensitivity values of MWCNT–NF–PMG film modified GCE toward the analytes are 1.3 mA mM^{-1} cm^{-2} for catechol and 0.9 mA mM^{-1} cm^{-2} for quinol. The correlation coefficients are 0.9536 and 0.9757 for catechol and quinol, respectively. Comparing these sensitivity values with those obtained in CV studies reveals that the DPV technique possesses higher sensitivity than the CV technique. In DPV, the calculated LODs at MWCNT–NF–PMG are 2.5 μM for catechol and 3.5 μM for quinol individually.

Fig. 5 shows the differential pulse voltammograms obtained during the simultaneous change of concentrations of catechol and quinol mixture at MWCNT–NF–PMG film modified GCE. The differential pulse voltammograms were recorded at a constant time interval of 2 min with nitrogen purging before the start of each experiment. The electroanalytical values from DPV such as linear range, slope and its correlation coefficient, standard error of slope, LOD, and LOQ for the analyte mixture at MWCNT–NF–PMG film are given in Table 3. From the slope values, the sensitivity values of MWCNT–NF–PMG film modified GCE toward the analyte mixture are 0.4 mA mM^{-1} cm^{-2} for catechol and 3.2 mA mM^{-1} cm^{-2} for quinol. The above-mentioned electroanalytical values are better than the previously reported values for the simultaneous determination of catechol and quinol [4,6–8]. Similarly, Table 4 shows a comparison of MWCNT–NF–PMG film (electrochemical method) with other techniques and reveals that most determinations were carried out for catechol or quinol but not in the mixture.

Fig. 6 exhibits the differential pulse voltammograms obtained for the different concentrations of catechol in the presence of 708.2 μM quinol at MWCNT–NF–PMG film modified GCE in pH 1.5 H_2SO_4 solution. The differential pulse voltammograms were recorded at a constant time interval of 2 min with nitrogen purging

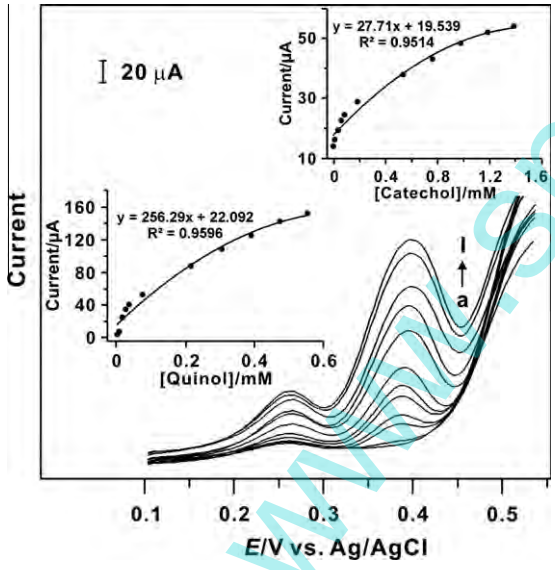

Fig.5. Differential pulse voltammograms of catechol and quinol present in analyte mixture (0.01–1.4 mM for catechol and 0.004–0.6 mM for quinol) at MWCNT–NF–PMG in pH 1.5 H_2SO_4 solution. The insets show the plots of peak current versus concentration of catechol (upper right) and quinol (lower left).

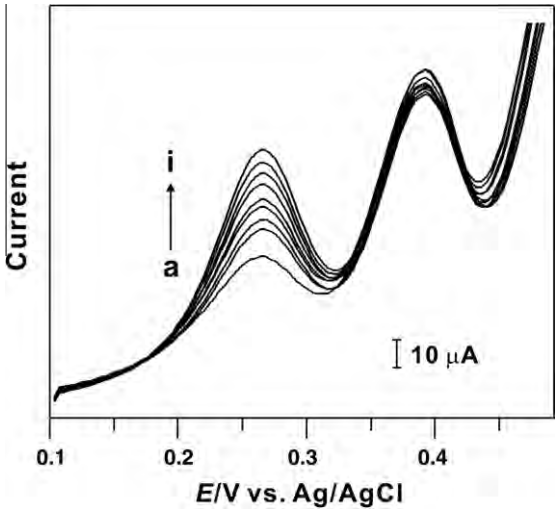

Fig.6. Differential pulse voltammograms of MWCNT–NF–PMG composite film shown in the presence of 708.2 μM quinol with increasing concentrations of catechol from 0.5 mM (a) to 1.8 mM (i) in pH 1.5 H_2SO_4 solution.

Table 4
Comparison detection limit values of catechol and quinol obtained in various techniques.

Technique	Analyte	LOD	References
Electrochemical using MWCNT–NF–PMG	Mixture of catechol and quinol	5.8/1.6 μM	This work
Belousov–Zhabotinskii-type oscillating system	Catechol	2.1 μM	[45]
Use of catecholoxygenase	Catechol	5 μM	[46]
Titrimetric	Catechol	20 μg	[47]
Spectrophotometric	Catechol	5 μg	[47]
Polarographic	Catechol	1 μg	[47]
High-performance liquid chromatography	Quinol	0.278 μg ml^{-1}	[48]
Second ratio spectra derivative spectrophotometry	Mixture of catechol and quinol	0.01009 mg ml^{-1}	[49]

before the start of each experiment. The voltammetric peak corresponding to the oxidation of catechol increases linearly with the increase in the concentration of catechol, whereas the peak current for oxidation of quinol decreased slightly as the number of cycles increased. This result reveals that there is not much interference between catechol and quinol. From the above DPV results, it is obvious that MWCNT–NF–PMG composite film modified GCE is suitable and efficient for the simultaneous detection of catechol and quinol.

Conclusions

A composite material that is highly stable in pH 1.0–4.0 aqueous solutions has been developed using MWCNTs, NF, and PMG at GCE, gold, and ITO electrodes. The developed MWCNT–NF–PMG composite film for the electrocatalysis combines the advantages of ease of fabrication and sufficient stability. The EQCM results confirmed the incorporation of PMG on MWCNT–NF modified electrode. The AFM results showed the morphological differences among MWCNT–NF film, NF–PMG film, and MWCNT–NF–PMG composite film. Furthermore, it was found that MWCNT–NF–PMG composite film has excellent functional properties along with good electrocatalytic activity toward catechol and quinol. The experimental methods of CV and DPV with MWCNT–NF–PMG composite film integrated at the GCE presented in this article provide an opportunity for simultaneous determination of catechol and quinol. Therefore, this work has established and illustrated, in principle and potential, a simple and novel approach for the development of a simultaneous catechol and quinol voltammetric sensor based on MWCNT–NF–PMG composite film modified GCE.

Acknowledgment

This work was supported by the National Science Council and the Ministry of Education of Taiwan (Republic of China).

Appendix A. Supplementary data

Supplementary data associated with this article can be found, in the online version, at doi:10.1016/j.ab.2010.12.002.

References

[1] S.G. Wang, Y.Q. Li, X.J. Zhao, J.H. Wang, J.J. Han, T. Wang, Electrochemical detection of catechol at integrated carbon nanotubes electrodes, Diamond Relat. Mater. 16 (2007) 248–252.
[2] S. Mu, Catechol sensor using poly(aniline-co-*o*-aminophenol) as an electron transfer mediator, Biosens. Bioelectron. 21 (2006) 1237–1243.
[3] F.J. Anaissi, H.E. Toma, Catechol incorporation and detection using bentonite–vanadium(V) oxide xerogels, Sens. Actuators, B 110 (2005) 175–180.
[4] M.A. Ghanem, Electrocatalytic activity and simultaneous determination of catechol and hydroquinone at mesoporous platinum electrode, Electrochem. Commun. 9 (2007) 2501–2506.
[5] M.R. Carvalho, C. Mello, L.T. Kubota, Simultaneous determination of phenol isomers in binary mixtures by differential pulse voltammetry using carbon fibre electrode and neural network with pruning as a multivariate calibration tool, Anal. Chim. Acta 420 (2000) 109–121.
[6] H. Qi, C. Zhang, Simultaneous determination of hydroquinone and catechol at a glassy carbon electrode modified with multiwall carbon nanotubes, Electroanalysis 17 (2005) 832–838.
[7] J. Yu, W. Du, F. Zhao, B. Zeng, High sensitive simultaneous determination of catechol and hydroquinone at mesoporous carbon CMK-3 electrode in comparison with multi-walled carbon nanotubes and Vulcan XC-72 carbon electrodes, Electrochim. Acta 54 (2009) 984–988.
[8] D.-M. Zhao, X.-H. Zhang, L.-J. Feng, L. Jia, S.-F. Wang, Simultaneous determination of hydroquinone and catechol at PASA/MWNTs composite film modified glassy carbon electrode, Colloid Surf. B 74 (2009) 317–321.
[9] V.L. Finkenstadt, Natural polysaccharides as electroactive polymers, Appl. Microbiol. Biotechnol. 67 (2005) 735–745.
[10] C.P. McMahon, G. Rocchitta, S.M. Kirwan, S.J. Killoran, P.A. Serra, J.P. Lowry, R.D. O'Neill, Oxygen tolerance of an implantable polymer/enzyme composite glutamate biosensor displaying polycation-enhanced substrate sensitivity, Biosens. Bioelectron. 22 (2007) 1466–1473.
[11] H.A. Al Attar, A.P. Monkman, Effect of surfactant on water-soluble conjugated polymer used in biosensor, J. Phys. Chem. B 111 (2007) 12418–12426.
[12] K. Pu, B. Liu, Optimizing the cationic conjugated polymer-sensitized fluorescent signal of dye labeled oligonucleotide for biosensor applications, Biosens. Bioelectron. 24 (2009) 1067–1073.
[13] J.-C. Vidal, E. Garcia-Ruiz, J.-R. Castillo, Recent advances in electropolymerized conducting polymers in amperometric biosensors, Microchim. Acta 143 (2003) 93–111.
[14] R. Pauliukaite, M.E. Ghica, M. Barsan, C.M.A. Brett, Characterisation of poly(neutral red) modified carbon film electrodes: application as a redox mediator for biosensors, J. Solid State Electrochem. 11 (2007) 899–908.
[15] I. Becerik, F. Kadirgan, Glucose sensitivity of platinum-based alloys incorporated in polypyrrole films at neutral media, Synth. Met. 124 (2001) 379–384.
[16] T. Selvaraju, R.R. Ramaraj, Electrochemically deposited nanostructured platinum on Nafion coated electrode for sensor applications, J. Electroanal. Chem. 585 (2005) 290–300.
[17] M. Yasuzawa, A. Kunugi, Properties of glucose sensors prepared by the electropolymerization of a positively charged pyrrole derivative, Electrochem. Commun. 1 (1999) 459–462.
[18] C.P. Andrieux, O. Haas, J.M. Saveant, Catalysis of electrochemical reactions at redox-polymer-coated electrodes: mediation of the iron(III)/iron(II) oxido-reduction by a polyvinylpyridine polymer containing coordinatively attached bisbipyridine chlororuthenium redox centers, J. Am. Chem. Soc. 108 (1986) 8175–8182.
[19] J. Wang, M. Musameh, Electrochemical detection of trace insulin at carbon-nanotube-modified electrodes, Anal. Chim. Acta 511 (2004) 33–36.
[20] H. Cai, X. Cao, Y. Jiang, P. He, Y. Fang, Automated method for the determination of vitamin D_3 hydroxymetabolites in serum, Anal. Bioanal. Chem. 375 (2003) 287–292.
[21] A. Erdem, P. Papakonstantinou, H. Murphy, Direct DNA hybridization at disposable graphite electrodes modified with carbon nanotubes, Anal. Chem. 78 (2006) 6656–6659.
[22] H. Beitollahi, M.M. Ardakani, H. Naeimi, B. Ganjipour, Electrochemical characterization of 2,2′-[1,2-ethanediylbis (nitriloethylidyne)]-bis-hydroquinone–carbon nanotube paste electrode and its application to simultaneous voltammetric determination of ascorbic acid and uric acid, J. Solid State Electrochem. 13 (2009) 353–363.
[23] P. Gajendran, R. Saraswathi, Polyaniline–carbon nanotube composites, Pure Appl. Chem. 80 (2008) 2377–2395.
[24] E. Mendoza, J. Orozco, C. Jiménez-Jorquera, A.B. González-Guerrero, A. Calle, L.M. Lechuga, C. Fernández-Sánchez, Scalable fabrication of immunosensors based on carbon nanotube polymer composites, Nanotechnology 19 (2008) 1–6.
[25] J. Wang, J. Dai, T. Yarlagadda, Carbon nanotube–conducting-polymer composite nanowires, Langmuir 21 (2005) 9–12.
[26] Y. Zou, L. Sun, F. Xu, Prussian blue electrodeposited on MWNTs–PANI hybrid composites for H_2O_2 detection, Talanta 72 (2007) 437–442.
[27] C.-M. Chang, Y.-L. Liu, Functionalization of multi-walled carbon nanotubes with non-reactive polymers through an ozone-mediated process for the preparation of a wide range of high performance polymer/carbon nanotube composites, Carbon 48 (2010) 1289–1297.
[28] S.R. Ali, R.R. Parajuli, Y. Ma, Y. Balogun, H. He, Interference of ascorbic acid in the sensitive detection of dopamine by a nonoxidative sensing approach, J. Phys. Chem. B 111 (2007) 12275–12281.
[29] R.J. Chen, Y. Zhang, D. Wang, H. Dai, Noncovalent sidewall functionalization of single-walled carbon nanotubes for protein immobilization, J. Am. Chem. Soc. 123 (2001) 3838–3839.
[30] A.A. Karyakin, E.E. Karyakina, H.-L. Schmidt, Electropolymerized azines: a new group of electroactive polymers, Electroanalysis 11 (1999) 149–155.
[31] A.G. MacDiarmid, J.C. Chiang, A.G. Richter, A. Epstein, Polyaniline: a new concept in conducting polymers, Synth. Met. 18 (1987) 285–290.
[32] R. Mazeikiene, G. Niaura, O. Eicher-Lorka, A. Malinauskas, Raman spectroelectrochemical study of toluidine blue, adsorbed and electropolymerized at a gold electrode, Vib. Spectrosc. 47 (2008) 105–112.
[33] Q. Wan, X. Wang, X. Wang, N. Yang, Poly(malachite green) film: electrosynthesis, characterization, and sensor application, Polymer 47 (2006) 7684–7692.
[34] X. Wang, N. Yang, Q. Wan, X. Wang, Catalytic capability of poly(malachite green) films based electrochemical sensor for oxidation of dopamine, Sens. Actuators, B 128 (2007) 83–90.
[35] Y. Umasankar, A.P. Periasamy, S.M. Chen, Poly(malachite green) at Nafion doped multi-walled carbon nanotube composite film for simple aliphatic alcohols sensor, Talanta 80 (2010) 1094–1101.
[36] N. Darsono, D. Yoon, J. Kim, Milling and dispersion of multi-walled carbon nanotubes in texanol, Appl. Surf. Sci. 254 (2008) 3412–3419.
[37] J. Chen, A.M. Rao, S. Lyuksyutov, M.E. Itkis, R.E. Smalley, R.C. Haddon, Dissolution of full-length single-walled carbon nanotubes, J. Phys. Chem. B 105 (2001) 2525–2528.
[38] Y.C. Tsai, S.C. Li, J.M. Chen, Cast thin film biosensor design based on a Nafion backbone, a multiwalled carbon nanotube conduit, and a glucose oxidase function, Langmuir 21 (2005) 3653–3658.
[39] G.A. Rivas, S.A. Miscoria, J. Desbrieres, G.D. Barrera, New biosensing platforms based on the layer-by-layer self-assembling of polyelectrolytes on Nafion/

carbon nanotubes-coated glassy carbon electrodes, Talanta 71 (2007) 270–275.
[40] S.M. Chen, M.I. Liu, Electrocatalytic properties of NDGA and NDGA/FAD hybrid film modified electrodes for NADH/NAD^+ redox reaction, Electrochim. Acta 51 (2006) 4744–4753.
[41] S.M. Chen, C.J. Liao, V.S. Vasantha, Preparation and electrocatalytic properties of osmium oxide/hexacyanoruthenate films modified electrodes for catecholamines and sulfur oxoanions, J. Electroanal. Chem. 589 (2006) 15–23.
[42] E. Laviron, General expression of the linear potential sweep voltammogram in the case of diffusionless electrochemical systems, J. Electroanal. Chem. 101 (1979) 19–28.
[43] A. Mohadesi, M.A. Taher, Electrochemical behavior of naphthol green B doped in polypyrrole film and its application for electrocatalytic oxidation of ascorbic acid, Sens. Actuators, B 123 (2007) 733–739.
[44] U. Yogeswaran, S.M. Chen, Multi-walled carbon nanotubes with poly(methylene blue) composite film for the enhancement and separation of electroanalytical responses of catecholamine and ascorbic acid, Sens. Actuators, B 130 (2008) 739–749.
[45] P. Chen, G. Hu, W. Wang, J. Song, L. Qiu, H. Wang, L. Chen, J. Zhang, L. Hu, Determination of catechol based on an oscillating chemical reaction involving a macrocyclic complex as catalyst, J. Appl. Electrochem. 38 (2008) 1779–1783.
[46] B.Z. Egan, D.W. Holladay, Use of catecholoxygenase for determination of catechol, Anal. Lett. 10 (1977) 213–224.
[47] D. Amin, S.T. Sulaiman, Titrimetric, spectrophotometric, and polarographic determination of resorcinol, catechol, and phloroglucinol, Analyst 109 (1984) 739–741.
[48] T.B. Vree, A.J. Lagerwerf, C.P. Bleeker, P.M. de Grood, Direct high-performance liquid chromatography determination of propofol and its metabolite quinol with their glucuronide conjugates and preliminary pharmacokinetics in plasma and urine of man, J. Chromatogr., B 721 (1999) 217–228.
[49] J. Liu, Z. Lin, Simultaneous determination of mixed phenol, catechol, and quinol by double Fourier transform filtering and second ratio spectra derivative spectrophotometry, Guang Pu Xue Yu Guang Pu Fen Xi (Spectrosc. Spectral Anal.) 20 (2000) 480–483.